International Journal of Astronomy 2012, 1(4): 62-67
DOI: 10.5923/j.astronomy.20120104.02

Spectral Energy Distributions and Age Estimates of Five Massive Young Stellar Objects

Kamal Kumar Tanti[1,*], Jayashree Roy[2], Kalpana Duorah[1]

[1]Department of Physics, Gauhati University, Guwahati, 781014, India
[2]Indian Institute of Astrophysics, Bangalore, 560034, India

Abstract We present the spectral energy distributions (SEDs) of five massive young stellar objects (YSOs), detected from the NIR imaging survey carried out by Varricatt et al.[1] and estimated the physical and structural/geometrical parameters, including their ages and masses, for each of the five central YSO outflow candidates, along with their associated circumstellar disks and infalling envelopes. The SEDs of YSOs in five massive star forming regions has been reconstructed using 2MASS, MSX, IRAS, IRAC & MIPS, SCUBA, WISE, SPIRE and IRAM data, partly available from previous works, using the on-line SED Fitting tool developed by[2],[3]. We have derived the IRAS catalogue fluxes as well as the fluxes in the Mid-IR and sub-mm/mm, directly from the images. With the help of the analysis of SEDs and subsequently estimated parameters for the central YSO sources along with its circumstellar disks and envelopes, the cumulative distribution of the stellar ages and masses of the massive YSOs can be analysed. This leads to a better understanding for the formation history of massive stars in their respective star forming regions.

Keywords Stars: Massive, Stars: Pre-Main-Sequence, Radiative Transfer, SED, SED Fitting Tool

1. Introduction

Massive stars (with mass $M \geq 8\ M_{\odot}$) form in the dense, optically thick cores of molecular clouds throughout the galaxy. Massive stars play a vital role in shaping the galactic structure as well as in the dynamical evolution of the Universe, by producing UV radiation and heavy elements that injects energy within the interstellar medium (ISM) and actively participating in the heating of the parental molecular clouds, thereby regulating the rate of star formation. During their short life time, they undergo a number of physical processes and an evolutionary sequence, starting from pre-stellar cores to main-sequence stars.

By the combined effects of stellar winds, massive bipolar outflows, expanding HII regions, and supernova explosions, massive stars play a key role in mixing and turbulence in the ISM of galaxies. The formation and evolution of massive stars thus not only profoundly affect the star-formation process as a whole along with the planet formation process, but also plays an active role in determining the physical, chemical and morphological structures of galaxies. Thus massive stars are a link between stellar, galactic and cosmic evolutions. Though luminosity of massive stars enables a complete census of their formation processes that take place in the galaxy, still the formation and early evolution of massive stars are not well-understood.

The formation and the initial stages of the evolution of massive stars mainly deal with the protostars/young stellar objects (YSOs) in the dense environment of interstellar dust and gas within the parental molecular cloud. In this dusty environment, the YSOs and protostars are embedded by the dense circumstellar dust and molecular gas that absorbs the stellar radiation and re-emits it to wavelengths long wards than 1 μm[4]. According to Lada[4], the proto- stars have a spectral energy distribution (SED) with a positive slope in the 2-20 μm spectral range. By the shapes of the SEDs, Lada first classified pre-main sequence (PMS) stars into an evolutionary sequence, Classes I through III, based on the values of intervals of spectral index, α. Later Greene et al. in 1994[5] added a fourth class of "flat spectrum" class sources, an earlier stage, Class 0, which are more deeply embedded sources. This has been proved for low mass YSOs[6]. The case for young massive stars is topic of recent investigation[7].

The study of the circumstellar environment of YSOs is very crucial to understand the pre-main sequence (PMS) evolution processes of massive stars. For this purpose, the multi-wavelength photometry and analysis can be done and subsequently, the spectral energy distributions (SEDs) can be constructed, by calculating the radiation transfer models, considering a central source and given circumstellar dust and gas geometry, as well as dust properties, and thus estim

* Corresponding author:
research.kamal@gmail.com (Kamal Kumar Tanti)
Published online at http://journal.sapub.org/astronomy

ating a set of parameters that reproduce the observations. By this way, all the physical and structural/geometrical parameters of a central YSO outflow candidate, along with their associated circumstellar disk and infalling envelope, can be estimated. This will help us in understanding the physical and structural evolution of pre-main sequence (PMS) stars, thereby identifying the evolutionary status of the central source as well as the disks & envelopes that will provide is a better understanding of massive star formation processes.

2. Radiative Transfer Modeling and SED Fitting Tool

In order to analyse and characterize the physical/geometrical properties and the evolutionary track of disks & envelopes around all the selected five massive young stellar objects (MYSO), the SEDs of YSOs were constructed and modelled using on-line SED Fitting Tool of[3], that uses a grid of 2D radiative transfer models presented in[2], developed by[8] ,[9].

Robitaille et al. I & II ([2],[3]) presented a grid of 2D radiative transfer models of axisymmetric YSOs, covering a wide range of stellar masses (from 0.1 $M_{\odot}$ to 50 $M_{\odot}$) and evolutionary stages (from the early envelope infall stage to the late disk-only stage).

A Monte-Carlo radiation transfer code is used for computing the model SEDs, for 20,071 different sets of physical parameters (e.g. stellar mass, disk mass, envelope infall rate, etc...), and for 10 viewing angles. Thus this 2D radiative transfer grid consists of 20,071 YSO models, with SEDs and polarization spectra computed at 10 viewing angles for each model, resulting in a total of 200,710 SEDs.

Each of the 20,071 sets of physical parameters is referred to using a 7 digit number in the form of 30xxxxx. For each of these sets of parameters, SEDs are available for 10 viewing angles and for 50 different apertures between 100 and 100,000AU.

The radiation transfer modeling has been carried out for the selected YSO candidates, to extract the various physical parameters for the particular star-forming region, using the SED fitting tool, available online. All the available data for the given sources, in different wavelength bands, are fitted using the tool, and thus a best-fit YSO SED plot is obtained for every YSO source.

Generally, with this technique, the top 10 YSO SED fits can be obtained for a given source, at the same aperture, and different χ^2 (Total) & A_v values, as well as different viewing angles. These top 10 YSO SED models correspond to the SEDs at the correct viewing angle and at the same aperture. The first of the top 10 YSO SED models, with less χ^2 (Total) value has been considered, as this model gives the best-fit YSO SED model for the given source.

To obtain better results for constructing SEDs for all five sources, we derived, compiled and used all the available NIR, MIR and FIR data, e.g., 2MASS J-H-K_s band data, magnitudes in the Spitzer IRAC bands 1-4 & MIPS bands 1-2, IRAS 12, 25, 60, 100-μm data, MSX Bands A, C, D & E data, SCUBA 450 & 850-μm data, WISE 3.4, 4.6, 12, 22-μm data, SPIRE 250, 350, 500-μm data and the IRAM 1.2 mm data.

3. Selection of MYSOs

For our current analysis, the massive young stellar outflow candidates are selected from the NIR imaging survey carried out by[1]. The reason for selecting these outflow candidates is that bipolar molecular outflows have long indicated that accretion discs are present at the heart of massive star formation. Varricatt et al.[1] had selected those candidates that are young, high-mass objects with evidence of outflows.

In the following sections, we will discuss, in detail, about all the five massive young stellar objects (MYSOs).

3.1. IRAS 06061+2151

IRAS 06061+2151 (AFGL 5182) is one of the most massive star forming region located in the Gemini OB1 cloud complex and in the Perseus spiral arm[10]. Its photometric distance is 2.0 kpc[10]. There are strong indications of star formation activity in this deeply embedded region, in the extended (~1 pc) and massive (~ 7000 $M_{\odot}$) molecular cloud complex observed in $C^{18}O$ line emission[11]. There is a compact cluster, AFGL 5182, at the centre seen in near-infrared (NIR)[10].

There are several sources associated with IRAS 06061+2151: (a) a radio continuum source associated with the ultra-compact HII (UCHII) region, G188.794+1.031, (b) a sub-millimeter wavelength source, JCMTSF J060907.1+215037, (c) a near infrared (NIR) cluster GL 5182 detected in the $C^{18}O$ line emission ([11],[12]). The UCHII region is extremely young as its ionization source is still in the accretion phase[13]. Moreover, this region shows the H_2O maser emission[13]. Thus the structure and the kinematics of a molecular gas around this region have been well studied with high spatial resolution observations. Motogi et al.[13] found the bipolar morphology and the expanding motion suggested by the relative proper motion measurement of H_2O masers.

Anandarao et al.[14] detected a young stellar object with an evidence of outflow in the form of knot-like structure, which suggests a protostellar jet, towards the massive star forming region IRAS 06061+2151, in the molecular hydrogen emission line (2.121 mm). Near-infrared images reveal that IRAS 06061+2151 is a cluster of at least five sources, four of which seem to be early B-type young stellar objects, in a region of 12 arcsec surrounded by a nebulosity. A new source S5 appears to have a very steep infrared energy distribution and is likely a massive proto-star as its colors (lower limits) suggest a heavily embedded source. The H-K_s/J-H color-color diagram indicates that it is a Class I type pre-main sequence (PMS) star[14].

3.2. IRAS 19110+1045

IRAS 19110+1045 (G45.07+0.13) is a known UCHII region and having luminosity of (330; 588.8) $\times 10^3$ $L_\odot$ at a distance of (6; 8.3; 9.7 kpc)[15]. The extent of ionised gas of the HII region IRAS 19111+1045 is ~ 1.3 pc[15].

Hunter et al.[16] first detected bipolar molecular outflows from this source. Their CO (J=6-5) map shows an unresolved bipolar molecular outflow (beam size ~ 10 arcsec), with its origin well centred on the radio position of the UCHII region. The estimated mass of the outflow is 45 $M_\odot$ and the length is 0.3 pc. The existence of H_2O maser emission from this source is believed to trace the earliest stages of star formation and on the compactness of the source (appeared to contain a single core). Hunter et al.[16] argued that G45.07+0.13 is a younger source than the nearby G45.12+0.13.

Extended radio emission is detected around IRAS 19110+1045, which contains Type I OH masers as well as H_2O maser. Methyl cyanide also has been detected towards this UCHII region[17].

3.3. IRAS 20188+3928

Little et al.[18] mapped IRAS 20188+3928 in HCO^+ and CO emission lines and discovered a dense bipolar molecular outflow associated with this source in the N-SW direction that indicates that it is an active region for massive star formation.

Bronfman et al.[19] detected the source in CS(2-1) line emission for this source. The detection of NH_3 emission signifies that this region is deeply embedded. NH_3 observations by Anglada et al.[20] showed a velocity gradient indicating entrainment by high velocity gas. They also detected a variable H_2O maser ~ 1 arcmin in the NW of the IRAS position.

Molinari et al.[21] detected two-component 6-cm emission using the VLA, with the stronger component (29.95 mJy) within one arcsec of the IRAS position and agreeing with the position of the brightest radio source of[22] and the weaker one (3.82 mJy) located ~ 21 arcsec NE, and agreeing in position with the northern radio source[22]. The distance estimated to this source varies from 0.31 to 4 kpc ([18]). Accordingly, the luminosity also is highly uncertain, e.g., between 0.343×10^3 $L_\odot$ to 52.8×10^3 $L_\odot$.

Zhang et al.[23] observed a bipolar molecular outflow in CO emission, centred on the IRAS source and roughly in the NS direction, which is consistent with the H_2 emission. The outflow in CO is better centred on the illuminating source ~ 6 arcsec north of the IRAS position[23].

Near-IR images by Varricatt et al.[1] show a cluster of deeply embedded objects towards the centre of the field, very close to the IRAS position. The faint radio peak ~ 20 arcsec north of the IRAS position was detected by[21] and[22]. This radio emission is likely to be from a highly embedded source. The presence of the radio sources and the outflows implies that there are multiple YSOs in the region, which are likely to be at different stages of evolution.

3.4. IRAS 20198+3716

IRAS 20198+3716 (ECX6-7b) coincides with the extensive and active star forming region ON2 that extends over roughly ~ 15 pc at a distance of 5.5 kpc. ON2-N (the northern region, referred to as ON2-N by[24]) contains the UCHII region G75.78+0.34, while the southern cloud contains the HII region G75.77+0.34. The location of the latter is close to the IRAS position. The location of the ON2-S is further south-east of the IRAS position by ~ 30 arcsec, which is close to their spatial resolution.

Shepherd et al.[24] studied ON2 in 3-mm continuum emission, CO, SiO, $H^{13}CO^+$ and SO_2, at high spatial resolution and found evidence for at least four molecular outflows. Water and Methanol masers are observed at various locations throughout the region[25], whereas water maser emission closely associated with the northern source.

Dent et al.[26] derived a late O spectral type for the southern HII region HIIS (G75.77+0.34) and an early B spectral type for HIIC (G75.78+0.34; ON2-N of[24]). Shepherd et al.[24] resolved 4-mm continuum sources in this region, where H_2O and OH masers are detected. Also, a cometary UCHII region is detected with an integrated flux density of ~ 40.4 mJy at 6 cm.

Together, these observations imply that this is a region with very active star formation. The YSOs drive the outflow that we observe in H_2, while more evolved, luminous objects ionize the circumstellar medium.

3.5. IRAS 20293+3952

IRAS 20293+3952 is a massive star forming region with the presence of dense core, where active star formation is going on. Beuther et al.[27] detected a dense core in CS and 1.2 mm dust continuum emission ~ 23 arcsec to the east and 3.4 arcsec north of the IRAS position. They also detected a much fainter peak located NW of the IRAS position. The bright mm continuum peak was resolved into three at 1.3 mm and 3 mm using high angular resolution interferometric observations using PDBI. High resolution CO and SiO maps of Beuther et al.[28] resolve four outflows in this region. A water maser is detected towards the dust core and outflow source, while a resolved 3.6-cm radio continuum source with an integrated flux density of 7.6 mJy is detected toward the IRAS position suggesting the presence of an HII region ([28],[29]). Sridharan et al.[29] also detected the hot-core tracers CH_3OH and CH_3CN towards the IRAS source. Sridharan et al.[29] did not find any evidence for the presence of 6.7-GHz methanol maser. They detected strong H_2O maser, located close to the dust continuum peak.

Kumar et al.[30] present near-IR images of IRAS 20293+3952; they detect H_2 emission coincident with the blue-shifted CO lobe, as well as compact features to the NE and SE. They also observed a ring of H_2 emission surrounding one of the two bright near-IR sources in the cluster near the IRAS position. Deep infrared photometry and spectroscopy are needed to study the cluster around this

source, to identify the outflow driving sources and to understand the nature of H_2 ring/shell.

4. Results and Discussion

As massive stars form and evolve following an evolutionary sequence, physical and structural properties of YSOs also evolve. Fitting their SEDs can provide us these properties, which can give us insights to understand the physical and structural evolution of pre-main sequence (PMS) stars as well as the evolution of star clusters where these massive stars were born.

The physical properties of the central source, such as effective temperature and luminosity, are the most important parameters in understanding the evolutionary status of the central source, and play a crucial role in the physical properties of disks and envelopes, because dust in the disks and envelopes are heated by irradiation from the star as well as from accretion shocks at the stellar surface.

In this study, the spectral energy distributions (SEDs) of five massive YSO outflow candidates are presented and all the physical and structural/geometrical parameters of all the YSO outflow candidates, along with their associated circumstellar disks and infalling envelopes, are estimated. Using this analysis, we can identify the evolutionary status of the central YSO source along with its disk and envelope. In this way, the physical and structural evolution of pre-main sequence (PMS) stars can be mapped.

We present the best-fit model SEDs for all the five selected massive YSO outflow sources, viz. IRAS 06061+2151, IRAS 19110+1045, IRAS 20188+3928, IRAS 20198+3716 & IRAS 20293+3952, as shown in the Figures 1-5, respectively.

The following are the salient features and results of our current analysis of constructing spectral energy distributions and subsequent estimation of different parameters of central YSO sources as well as their corresponding disks and circumstellar envelopes:

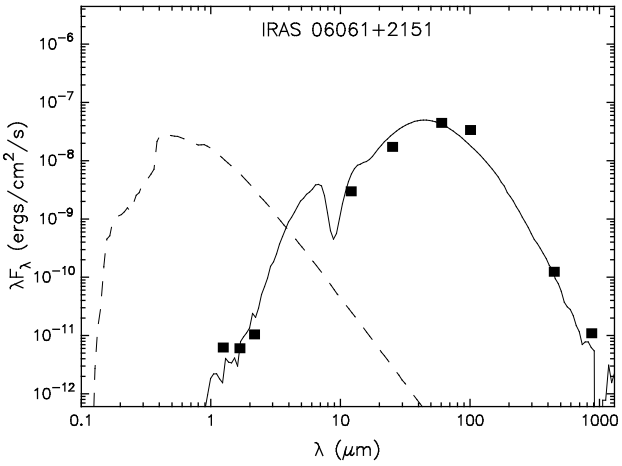

Figure 1. The Best-fit model SED for IRAS 06061+2151

(a) IRAS 06061+2151 is an active star forming region that has stellar mass 11.21 $M_\odot$, stellar temperature of 8,479 K, stellar age 2.89×10^4 yr and stellar radius 31.85 $R_\odot$. The central YSO source is surrounded by a 1.75×10^{-2} $M_\odot$, 97.5 AU disk with an accretion rate of 1.07×10^{-6} $M_\odot$/yr and a 60.9 $M_\odot$, 4.96×10^4 AU envelope with an accretion rate of 2.65×10^{-4} $M_\odot$/yr, viewed at an inclination angle of $i = 56.6^0$. The total luminosity has been estimated to be 4.72×10^3 $L_\odot$. The interstellar extinction necessary for this model to fit the data is $A_v = 88.4$ mag. The corresponding best-fit model SED is shown in Figure 1.

(b) IRAS 19110+1045 is high-mass young stellar object where there are constant activities of star formation going on. The estimated stellar parameters are: stellar mass ~ 28.60 $M_\odot$, stellar temperature ~ 14,052 K, stellar age ~ 5.74×10^3 yr, total luminosity ~ 1.01×10^5 $L_\odot$ and stellar radius ~ 53.62 $R_\odot$. The central YSO source is surrounded by a 4080 $M_\odot$, 1.01×10^5 AU envelope with an accretion rate of 9.71×10^{-3} $M_\odot$ /yr; viewed at an inclination angle of $i = 18.2^0$. The interstellar extinction is $A_v = 89.4$ mag. The corresponding best-fit model SED is shown in Figure 2.

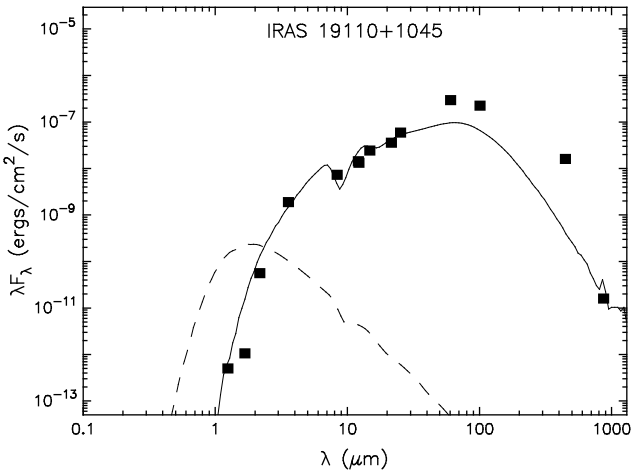

Figure 2. The Best-fit model SED for IRAS 19110+1045

(c) The SED fitting tool gives a stellar mass of 9.87 $M_\odot$, stellar radius of 37.72 $R_\odot$, stellar temperature of 6,785 K and a total luminosity of 2.74×10^3 $L_\odot$ for the YSO central source, IRAS 20188+3928. The stellar age is estimated as 3.17×10^4 yr and the interstellar extinction for fitting this model is $A_v = 2.24\times10^4$ mag. The disk parameters, viz., disk mass, disk radius and disk accretion rate are measured as 0.109 $M_\odot$, 108 AU, and 4.33×10^{-6} $M_\odot$/yr respectively. The parameters of envelope that surround the central source are calculated as: envelope mass ~ 36.4 $M_\odot$, envelope radius ~ 9.06×10^4 AU and envelope accretion rate ~ 4.59×10^{-5} $M_\odot$/yr. The corresponding best-fit model SED is shown in Figure 3.

(d) IRAS 20198+3716 is a massive YSO candidate with active star formation activity, that has stellar mass 8.99 $M_\odot$, stellar temperature of 24,325 K, stellar age 9.80×10^5 yr, total luminosity 4.31×10^3 $L_\odot$ and stellar radius 3.70 $R_\odot$. The central YSO source is surrounded by a 24.0 $M_\odot$, 1.00×10^5 AU envelope with an accretion rate of 1.43×10^{-7} $M_\odot$ /yr, viewed at an inclination angle of $i = 87.1^0$. The disk parameters are estimated as: disk mass ~ 6.66×10^{-2} $M_\odot$, disk radius ~ 580 AU and disk accretion rate ~ 1.29×10^{-7} $M_\odot$ /yr.

The interstellar extinction necessary for this model to fit the data is A_v = 9800 mag. The corresponding best-fit model SED is shown in Figure 4.

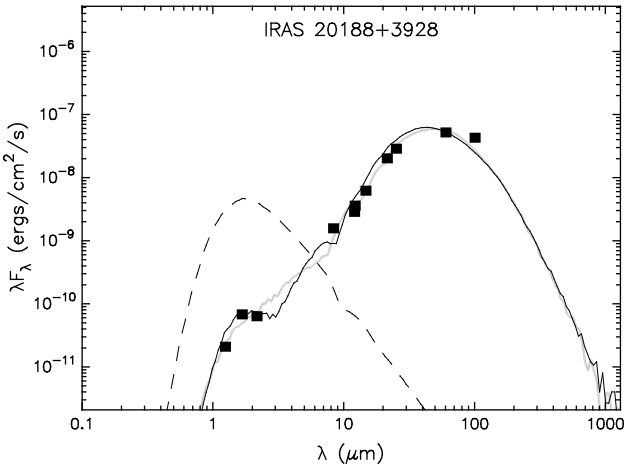

Figure 3. The Best-fit model SED for IRAS 20188+3928

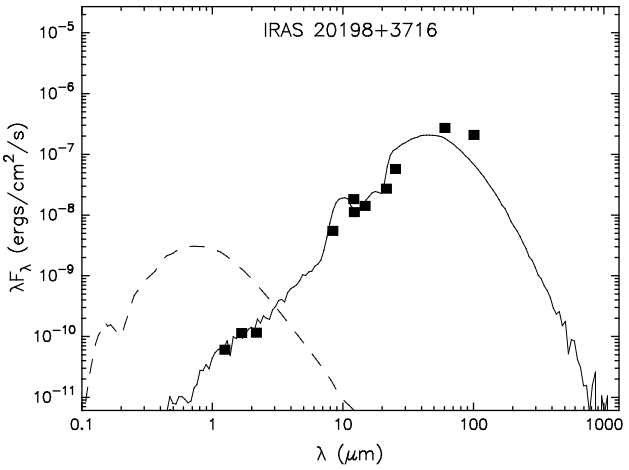

Figure 4. The Best-fit model SED for IRAS 20198+3716

(e) IRAS 20293+3952, that shows a constant star formation activity within its dense core, has a stellar mass of 10.91 $M_\odot$, stellar radius of 53.61 $R_\odot$, stellar temperature of 6,198 K and a total luminosity of 3.83×10^3 $L_\odot$. The stellar age of this MYSO is estimated as 2.03×10^4 yr and the interstellar extinction for fitting this model is A_v = 184 mag. The disk parameters, viz., disk mass, disk radius and disk accretion rate are measured as 1.01×10^{-1} $M_\odot$, 62.4 AU, and 3.07×10^{-6} $M_\odot$/yr respectively. The parameters of the envelope that surround the central source are calculated as: envelope mass ~ 80.2 $M_\odot$, envelope radius ~ 6.28×10^4 AU and envelope accretion rate ~ 2.33×10^{-4} $M_\odot$/yr. The corresponding best-fit model SED is shown in Figure 5.

Thus, the stellar mass of the target massive YSOs range between 8.99 $M_\odot$ to 28.60 $M_\odot$. The stellar temperatures of the sources are ranging between 6,198 K and 24,325 K. The stellar ages of all the sources are calculated, that ranges between 5.74×10^3 yr and 9.80×10^5 yr. The stellar radius of the selected YSOs ranges between 3.70 $R_\odot$ to 53.62 $R_\odot$. This analysis provides us a better understanding of the physical and structural evolution of the target massive YSO candidates within their respective star-forming regions.

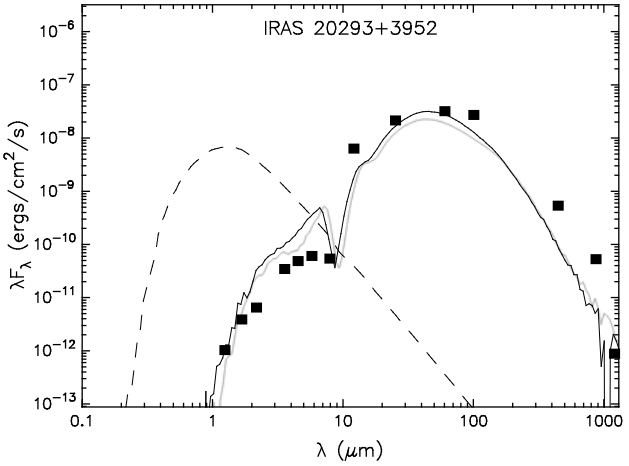

Figure 5. The Best-fit model SED for IRAS 20293+3952

In developing the 2D radiative transfer grid, Robitaille et al.[2] makes an assumption that there is an accretion scenario for the star formation process, in which a central star/YSO source is surrounded by an accretion disk, an infalling flattened envelope and bipolar cavities. Robitaille et al.[3] successfully tested this tool; but at the same time, it was observed that even if a number of SEDs in the model SED grid fit an observed SED, this does not mean that any of these models are actually the correct ones for the object in question. It only tells us that they are consistent with the observations.

Also, it may not always give meaningful result when we consider various scenarios of massive star formation (i.e., monolithic collapse, competitive accretion and stellar mergers). Although the SED models are more consistent with the monolithic collapse theory, but at the same time it is also consistent with the competitive accretion scenario. Thus, using this tool does not favour one of these formation scenarios over the other. To distinguish these formation scenarios, we would require a critical comparison of the SED models for all three scenarios and currently, this is not possible by using the current grid of models.

The online SED-fitting tool requires a minimum of three good quality data points. But still, we generally needed a larger set of data, spread over the wavelength region of 0.5 to 1000 μm, and then only we can get the SED model better constrained to yield better results, with least possible standard deviations. Also, in the online tool, we need to give the distance to the source and visual extinction as input parameters, which are usually a range of values. This leads to a further degeneracy of the SED models.

5. Conclusions

In this paper, we presented all the physical and structural/geometrical parameters of all the five massive YSO outflow candidates, along with the associated circumstellar disks and envelopes, obtained with the help of SED Fitting Tool. Also, the best-fit model SEDs for all the five selected massive YSO outflow sources are being presented in this paper which will help us in understanding

the physical and structural evolution of pre-main sequence (PMS) stars. Also, it explains self-consistently the embedded Young Stellar Objects (YSO) in dense interstellar clouds as well as the evolution of star clusters in the above massive star forming regions. This leads to a scenario for the formation history of massive stars in their respective star forming regions and subsequently, to a better understanding of the massive star formation processes in dense molecular clouds in our galaxy.

Future work will include the analysis of a larger perspective of massive star formation scenarios, for which we would select a large number of sources in a comparatively larger concentrated, dense area where there are constant activities of massive star formation. Also, the extraction of the possible YSO sources needs to be more articulate; thereby modeling the SEDs will provide more information about the possible point-like or clump-like appearance of the selected sources.

In that case, more coherent and consistent radiative transfer models such as, Whitney et al.[8] should be used for larger number of YSO sources and to perform this, the grid of 2D radiative transfer models of Robitaille et al. ([2],[3]) has to be extended in order to reproduce colder and earlier-stage objects. Also, a more critical definition of SED and a better SED fit will provide us with more reliable physical parameters of the YSOs in the dense galaxies; thereby presenting better comparisons with the theoretical models. Also while constructing the SEDs, a well-fit NIR data will provide the nature of the detected "cores". Another further outcome of the SED modeling is that the images can be produced at multiple wavelengths which would provide an insight to visualize what the future observatories will be capable of observing.

ACKNOWLEDGEMENTS

The authors would like to thank The Strasbourg astronomical Data Center (CDS), SIMBAD Astronomical Object Database and the VizieR Catalogue Service, available on-line. We are thankful to the anonymous referee for his/her critical comments and suggestions that greatly improved the presentation of the paper.

REFERENCES

[1] Varricatt, W.P., Davis, C.J., Ramsay, S.K. & Todd, S.P., MNRAS, 404, 661, 2010

[2] Robitaille, T. P., Whitney, B. A., Indebetouw, R., Wood, K., & Denzmore, P., ApJS, 167, 256, 2006

[3] Robitaille, T. P., Whitney, B. A., Indebetouw, R., & Wood, K., ApJS, 169, 328, 2007

[4] Lada, C. J., Star Forming Regions, IAU Symp. 115, ed. M. Peimbert & J. Jugaku (Dordrecht: Reidel), 1, 1987

[5] Greene, Thomas P.; Wilking, Bruce A.; Andre, Philippe; Young, Erick T.; Lada, Charles J., ApJ, 434, 614, 1994

[6] Hartmann, L., Megeath, S. T., Allen, L., Luhman, K., Calvet, N., D'Alessio, P., Franco- Hernandez, R., & Fazio, G., ApJ, 629, 881, 2005

[7] Zinnecker, H., & Yorke, H.W., ARA&A, 45, 481, 2007

[8] Whitney, B.A., Wood, K., Bjorkman, J.E., & Cohen, M., ApJ, 598, 1079, 2003

[9] Whitney, B.A., Wood, K., Bjorkman, J.E., & Wolff, M.J., ApJ, 591, 1049, 2003

[10] Carpenter, J. M., Snell, R. L., Schloerb F. P., ApJ, 450, 201, 1995

[11] Saito, H., Saito, M., Sunada, K., & Yonekura, Y., ApJ, 659, 459, 2007

[12] Di Francesco, J., Johnstone, D., Kirk, H., MacKenzie, T., & Ledwosinska, E., ApJS, 175, 277, 2008

[13] Motogi, K. et al., MNRAS, 390, 523, 2008

[14] Anandarao, B. G., Chakraborty A., Ojha D. K., Testi L., A&A, 421, 1045, 2004

[15] Vig, S., Ghosh S. K., Kulkarni V. K., Ojha D. K., Verma R. P., ApJ, 637, 400, 2006

[16] Hunter, T. R., Phillips, T. G., Menten, K. M., ApJ, 478, 283, 1997

[17] Pankonin,, V., Churchwell, E., Watson, C., & Bieging, J. H., ApJ, 558, 194, 2001

[18] Little, L. T., Bergman, P., Cunningham, C. T., Heaton, B. D., Knee, L. B. G., MacDonald, G. H., Richards, P. J., Toriseva M., A&A, 205, 129, 1988

[19] Bronfman, L., Nyman, L. A., May J., A&AS, 115, 81, 1996

[20] Anglada, G., Sepulveda, I., & Gomez, J. F., A&AS, 121, 255, 1997

[21] Molinari, S., Brand, J., Cesaroni, R., Palla, F., Palumbo, G. G. C., A&A, 336, 339, 1998

[22] Jenness T., Scott P. F., Padman R., MNRAS, 276, 1024, 1995

[23] Zhang, Q., Hunter, T. R., Brand, J., Sridharan, T. K., Cesaroni, R., Molinari, S., Wang J., Kramer, M., ApJ, 625, 864, 2005

[24] Shepherd, D. S., Churchwell, E., Wilner, D. J., ApJ, 482, 355, 1997

[25] Szymczak, M., Hrynek, G., Kus, A. J., A&AS, 143, 269, 2000

[26] Dent, W. R. F., MacDonald, G. H., Andersson, M., MNRAS, 235, 1397, 1988

[27] Beuther, H., Schilke P., Menten, K. M., Motte, F., Sridharan, T. K., et al., ApJ, 566, 945, 2002

[28] Beuther, H., Schilke, P., Gueth, F., ApJ, 608, 330, 2004

[29] Sridharan, T. K., Beuther, H., Schilke, P., Menten, K. M., Wyrowski, F., ApJ, 566, 931, 2002

[30] Kumar, M. S. N., Bachiller, R., Davis, C. J., ApJ, 576, 313, 2002